



HAL
open science

Atmospheric pressure plasmas for aerosols processes in materials and environment

J.P. Borra, N. Jidenko, E. Bourgeois

► **To cite this version:**

J.P. Borra, N. Jidenko, E. Bourgeois. Atmospheric pressure plasmas for aerosols processes in materials and environment. *European Physical Journal: Applied Physics*, 2009, 47 (2), pp.1-7. 10.1051/ep-jap/2009088 . hal-00486864

HAL Id: hal-00486864

<https://hal.science/hal-00486864>

Submitted on 27 May 2010

HAL is a multi-disciplinary open access archive for the deposit and dissemination of scientific research documents, whether they are published or not. The documents may come from teaching and research institutions in France or abroad, or from public or private research centers.

L'archive ouverte pluridisciplinaire **HAL**, est destinée au dépôt et à la diffusion de documents scientifiques de niveau recherche, publiés ou non, émanant des établissements d'enseignement et de recherche français ou étrangers, des laboratoires publics ou privés.

ATMOSPHERIC PRESSURE PLASMAS FOR AEROSOLS PROCESSES IN MATERIALS AND ENVIRONMENT

Borra JP, Jidenko N, Bourgeois E

*Laboratoire de Physique des Gaz et Plasmas CNRS-Univ. Paris-Sud, Orsay, F-91405
Supélec, 3 Rue Joliot Curie, Gif-sur-Yvette/, F-91192, France, jp.borra@pqp.u-psud.fr*

Abstract: The paper highlights applications of some atmospheric pressure plasmas (dc-corona, streamer and spark and ac-Dielectric Barrier Discharges) to aerosol processes for Materials and Environment (filtration, diagnostics).

The production of vapor i.e. condensable gaseous species, leads to nano-sized particles by physical and chemical routes of nucleation in these AP Plasmas: (i) when dc streamer and spark filamentary discharges as well as ac filamentary Dielectric Barrier Discharges interact with metal or dielectric surfaces, and (ii) when Discharges induce reactions with gaseous precursors in volume. It is shown how composition, size and structure of primary nano-particles are related to plasma parameters (energy, number per unit surface and time and thermal gradients).

Then the growth by coagulation controls the final size of agglomerates versus plasma parameters and transit time in and after the plasma. Charging and electro-thermal collection are depicted to account for the related potential applications of controlled kinematics of charged aerosol.

1. INTRODUCTION

Aerosol, defined as suspended liquid/solid particles (drop/powder) in gases, presents a large interfacial surface per unit volume used for heat exchanges, filtration and heterogeneous chemistry. More recently, nano-particles ($1D_{min} < 100nm$) have been synthesized for their physical properties (e.g. for tribological and mechanical properties of inorganic and carbon fullerenes) and for their chemical and bio-functionalities (e.g. for lower melting temperature, catalysis and drug delivery).

In gas phase, nano-sized aerosols are formed either by evaporation of liquid droplets leading to crystallized solute (spray drying and pyrolysis), or by gas-to-particle conversion (nucleation) when the saturation vapor pressure is overcome (as for crystallization above a saturation solute concentration).

Gas-phase aerosol processes performed at atmospheric pressure provide an economic alternative for nano-technologies. They are cost-effective, environment friendly (no liquid by-products) and energy efficient. Since, high-purity nanometer particles, more easy to collect from gases than from liquids, are produced, some aerosol processes are scaled-up for daily production of hundreds of tons of tailored TiO_2 particles and others are integrated in chemistry, energy, environment and health processes.

Production processes control particle size, composition and structure. Indeed, if nano-powders are used to save raw materials, the size-dependant properties of nano-materials are reported for tailored nano-particles, smaller than 50 nm with geometric standard deviation of the size distribution below 1,2 [1].

A post-production processing of particles (e.g. size selection, shaping of aggregates, mixing and homogeneous/focused deposition) leads to powders, composite materials, suspensions and coatings.

This paper focuses on the interest of dc to 100 kHz ac Atmospheric Pressure Electrical Discharges (hereafter referred as APED) for the production, the charging and the processing of aerosols. However, it does not cover processing of particles injected either in non-thermal Plasmas for functional coatings by post-discharge reactivity [2], nor in thermal plasmas for purification, spheroidisation, and surface coatings [3].

2. NANO-PARTICLE PRODUCTION BY NUCLEATION IN AP PLASMAS

Nucleation occurs when gaseous species are produced and saturated (partial pressure higher than the saturation vapor pressure). Two sources of vapor are depicted in AP Plasmas on Figure 1: (i) when dc filamentary streamer discharges as well as ac filamentary Dielectric Barrier Discharges interact with the metal or dielectric surface, and (ii) when the plasma induces reactions with gaseous precursors in volume. In both cases, condensable gaseous species lead to nanoparticles by physical and chemical routes of nucleation. It is shown how composition, size and structure of primary nanoparticles are related to plasma parameters (energy, number per unit surface and time and local thermal gradients). Then the growth by agglomeration controlling the final size of agglomerates is also related to plasma parameters as well as to the transit time in the plasma.

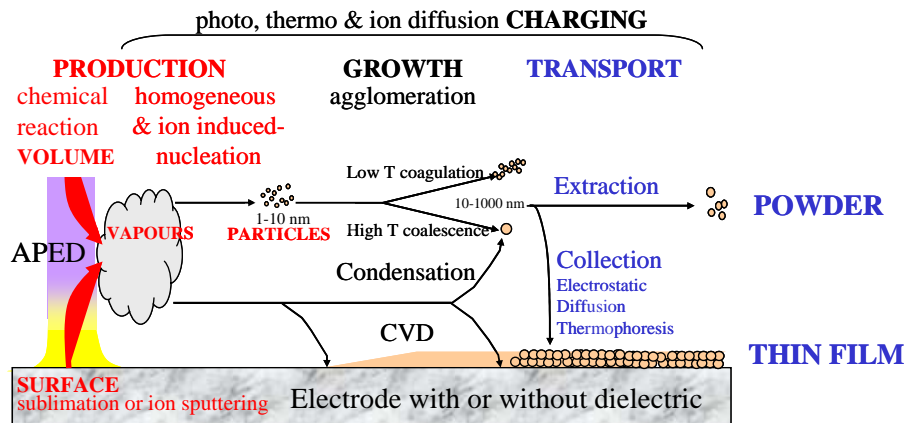


Figure 1: Mechanisms of vapor and particle production (nucleation), growth, charging and transport in APED [6]

2.1. Physical Nucleation

Vapors are produced by interaction of transient energy flux deposited by filamentary discharges on dielectric/electrode surface. Properties of primary nucleated nanoparticles can be controlled:

- Nature of the surface and of the gas controls the *final chemical composition of the nanoparticles*.
- Energy per filament produced in DBD depends on the gap geometry, the dielectric properties (gap length, specific capacitance depending on thickness and permittivity of dielectric material [4][5]), the relative humidity and controls the initial vapor flux from the surface and the *subsequent diameter of the primary nucleated nanoparticle* (cf. **Figure 2a**). The mass of material vaporized from the surface per filament is known to depend on the energy of the discharge filament [6]. That's the reason why we focus on the nucleation with « low energy » filamentary discharges to reduce vapor fluxes, local nucleated primary nanoparticles density and subsequent agglomeration, to prevent from larger size distributions and more dispersed related properties of such nano-powder produced in sparks (cf. § 2.3). Despite smaller energy per filament in DBD ($\sim \mu\text{J}$) than in spark, shorter duration (\sim nanosecond) and smaller surface ($\sim 10^{-5} \text{ cm}^2$) imply high surface power density ($\sim 10^{12} \text{ W.m}^{-2}$). The fluency threshold for vaporization (0.1 J.cm^{-2}) is reached and nucleation of vapors occurs close to each filament but leads to smaller particles than with spark, at concentrations below 10^7 cm^{-3} , as expected from the smaller vapor flux than with more energetic spark (cf. **Figure 2**, 3, 4 and 7).
- Thermal gradients around each filament, considered as a local and transient source of vapors, define the cooling rate of vapors by cold surrounding gas and the related *structure of the primary nucleated nanoparticle* (e.g. with spark in water [7]). Depending on the quenching rate, some unstable crystalline structures at STP can be produced (e.g. for fillers and low Temperature BaCO_3 for NO_x reduction [8]).

2.2. Reactive Nucleation

The chemical route of nucleation from gas-phase reactions is similar in flame and in plasmas [6]. In both cases, (i) condensable species are formed by gas-phase reactions between a gaseous precursor and reactive species formed in APED (e-, photon, excited species, radicals and ions, O_3 , NO_x , HNO_x), and (ii) the nucleated aerosol grows by simultaneous condensation and coagulation. Reactive

nucleation in low frequency DBD is mentioned here for gas pollution control on **Figure 2b** [9][10] and film deposition (cf. § 4.3, [11]). The reader can refer to [12] for Carbon nano-tube production. The high selectivity and vapors production rate through controlled kinetics of reactions in plasmas lead to high purity nanoparticles when a gaseous precursor is injected in the plasma [1][3][8][12].

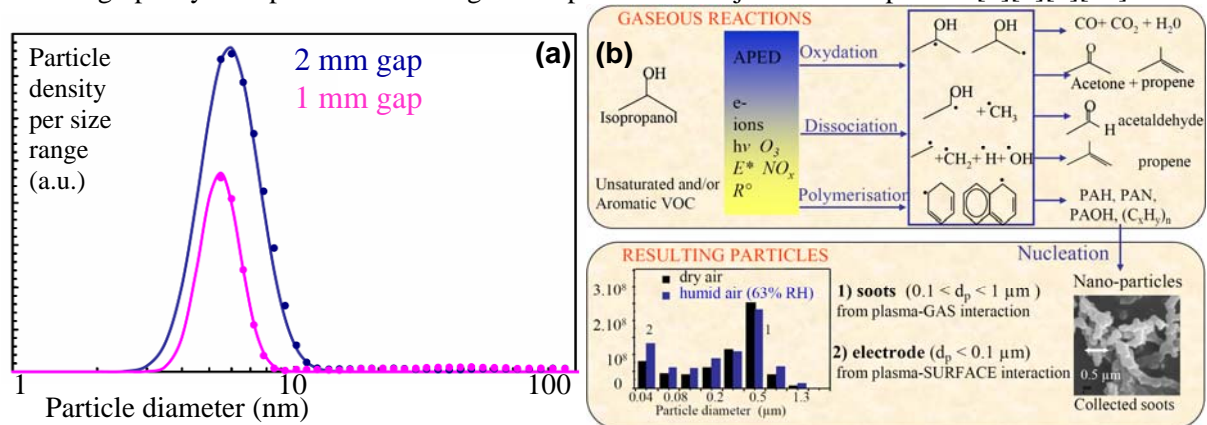


Figure 2: Size distributions of (a) SiO_x particles vs energy per filament for 1 or 2 mm DBD (5 mm glass at 70 kHz, 28 kV, 0.66 lpm N₂ with 150 ms maturation) ; (b) Gas-phase reaction with gaseous combustion by-product and particles in ac dbd treatment of 2000 ppmv toluene in air for 90 W injected in 300 l/h gas flow [6].

2.3. Dynamic of growth of primary nucleated nanoparticle into agglomerates by coagulation

Both filament-surface interaction in pure gases (no VOC traces) and gas-phase reactions with a precursor lead to intermediate transitory bimodal particle number size distributions corresponding to nucleation and agglomeration modes. The dynamics of particle formation by nucleation and of size evolution by coagulation are similar whatever the origin of the condensable species is. In both cases, nucleation occurs close to the vapor source leading to nanometer primary particles, which then coagulate within the plasma or in post-discharge maturation volume leading to agglomerates, as recently confirmed by [13]. Hence, the final size and properties (fractal dimensions and porosity) of agglomerates depend on the initial vapor flux and on the post-production growth and losses in the plasma reactor as well as in the eventual post-discharge maturation volume. Indeed, when aerosol measurements are performed after the reactor, the final size distribution depends on the size and density of primary nucleated nanoparticles, on the difference of gas and surface temperatures, on the transit times [11], and on the minimum size detected by the counter.

For instance in spark generators, the high energy per spark (from few mJ to J) leads to large particle diameter and high concentration (from 20 to 200 nm and 10^7 cm⁻³). Indeed, high particle concentration leads to particle growth by Brownian coagulation so that the initial bi-modal size distribution of nucleated and agglomerated nanoparticles turns into the so-called unimodal self preserving size distribution, as depicted on **Figure 3** [14][15]. Hence, « low energy » filamentary discharges reduce local vapor fluxes, nucleation rates and related primary nucleated nanoparticles concentration to control coagulation leading to narrower size distributions than in sparks.

Moreover, the porosity of agglomerates depends on the initial vapor flux and local thermal gradients, both related to the energy per discharge filament. Prevented sparks (from 0.5 to a few mJ per spark) at 200 Hz leads to similar aerosol size distribution and number concentration than the capacitive spark generator at 60 Hz with energy from 50 to 500 mJ per spark. Capacitive sparks produce mass concentration of Copper aerosol measured by Laser Induced Breakdown Spectroscopy above 100 μg.m⁻³, while prevented sparks produce lower mass concentration below the detection limit. Hence, agglomerates from prevented sparks are more porous than with more energetic capacitive sparks. This tends to confirm that much higher vapor flux, nucleation rate, and local primary nucleated nanoparticles density lead to faster coagulation and less porous agglomerates closer to the “high energy” capacitive spark than with less energetic prevented sparks. Besides, the post-production densification could also be induced in hotter gas close to capacitive sparks.

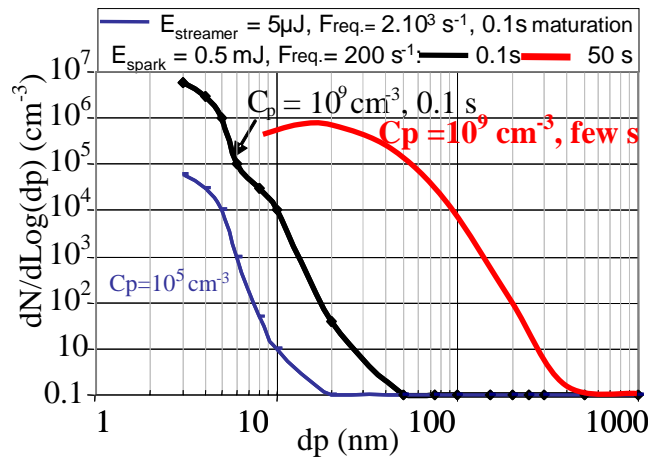


Figure 3 : Particles size distributions produced by APFD (a) in point-to-plane dc+ streamer and spark FD in clean and dry air, $d=1\text{cm}$ and $r_{\text{point}}=50\mu\text{m}$

With “low energy” filaments in DBD, **Figure 4a** and **b** show that the post-discharge number of particles per filament also depends on maturation time and that the size distribution seems unimodal. Indeed, the counter detects particles bigger than 5 nm. The increasing concentration with maturation time proves that coagulation of primary nanoparticles smaller than 5 nm also occurs to produce a self-preserving unimodal size distribution with modal diameter from a few to tens of nm, as shown on **Figure 4b**. For longer times, losses by diffusion reduce the number of particles per filament.

Besides, despite higher power density at 60 kHz than at 50 Hz, the productions per filament show similar trends and ranges with different maturation times. On the one hand, this confirms that charged species that would be collected at 50 Hz (cf. §3.2), do not represent an important part of outgoing particles; On the other hand, similar filaments in colder surrounding gases at 50 Hz than at 60 kHz, lead to faster nucleation and to higher particle concentration bigger than 5 nm, sooner after the DBD.

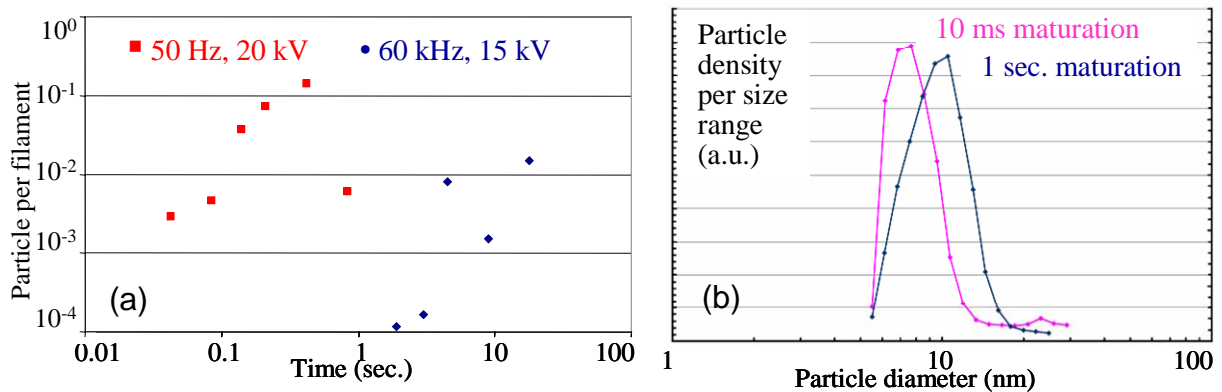


Figure 4 : (a) Number of particles per filament, for different post-discharge maturation time at 60kHz ($V_{\text{pp}}=15\text{ kV}$) and 50Hz ($V_{\text{pp}}=20\text{ kV}$); (b) Al_2O_3 particles vs maturation time (70 kHz, $V_{\text{pp}}=14\text{ kV}$, 0.5mm Al_2O_3 , 10 lpm)

3. AEROSOL CHARGING AND KINEMATICS OF CHARGED AEROSOLS

The analysis of forces on suspended particles shows that to deal with the sources of condensable gaseous species converted by nucleation into nanoparticles, the sinks of primary nanoparticles (losses to the wall -diffusion, thermophoresis and electro-collection-, as well as agglomeration) influences the final composition, structure and size of particles. Since charged aerosol kinematics depends mainly on electric forces, the charging mechanisms of submicron sized particles by collection of ions are presented in corona, post-corona and Dielectric Barrier Discharges. Indeed, in such defined electric field and ion densities profiles, both field and diffusion charging mechanisms account for the so-controlled kinematics of charged aerosols and for related applications (filtration, size distribution measurements, deposition).

3.1. Charging mechanisms

The charging mechanisms by collection of gaseous ions and the related charging laws are already defined. When particles get charged in gaseous ions/electrons densities “fine” particles smaller than 100 nm are mainly charged by diffusion of ions, “coarse” particles ($>1 \mu\text{m}$) are charged by the drift of ions on the field lines intersecting the surface of the particle, while in the intermediate size range (0.1 to $1 \mu\text{m}$) particles are charged by combined field and diffusion charging. For a given particle size, the particle charge level depends on both the electric field and the product of ion density (N_i, cm^{-3}) and transit time in this density (τ, s), as detailed in [6].

3.2. Comparison of corona and DBD chargers

APED are efficient aerosol chargers. Coronae are used on large voltage ranges due to high ion density in air/Nitrogen ($<10^9 \text{cm}^{-3}$). Diffusion charging [16][17], field charging [18], and combined charging laws [19] have been validated in stationary ion densities, especially in DC corona [20][21][22].

However, dc-corona chargers produce ozone and particles and leads to electro-collection [20][21][22] with related destabilization of the discharge. One way of limiting the losses is to work with lower voltage and lower related charge level; another is to use a post-discharge diffusion charging to reduce losses down to 50 % by self-electrostatic repulsion only, without discharge modification.

Figure 5a presents the measured mean number of charges per particle (points) versus particle diameter and theoretical diffusion and field charging laws (lines). In corona chargers, the mean $N_i\tau$ product (3.10^6 to 10^7s.cm^{-3}) is validated by Pauthenier and White or Fuchs’ charging laws, respectively for field charging of particles above $0.1 \mu\text{m}$ and for diffusion charging of smaller ones.

Higher numbers of charges per particle are reached in corona than in post-corona charger. Indeed both mechanisms occur in the first one whereas only diffusion charging leads to smaller charge levels in post-discharge. Indeed, in post-discharge diffusion chargers, the ion density is lower than in the corona gap and decreases from 10^6cm^{-3} by self-repulsion and electro-collection, inducing $N_i\tau$ product around 10^6s.cm^{-3} .

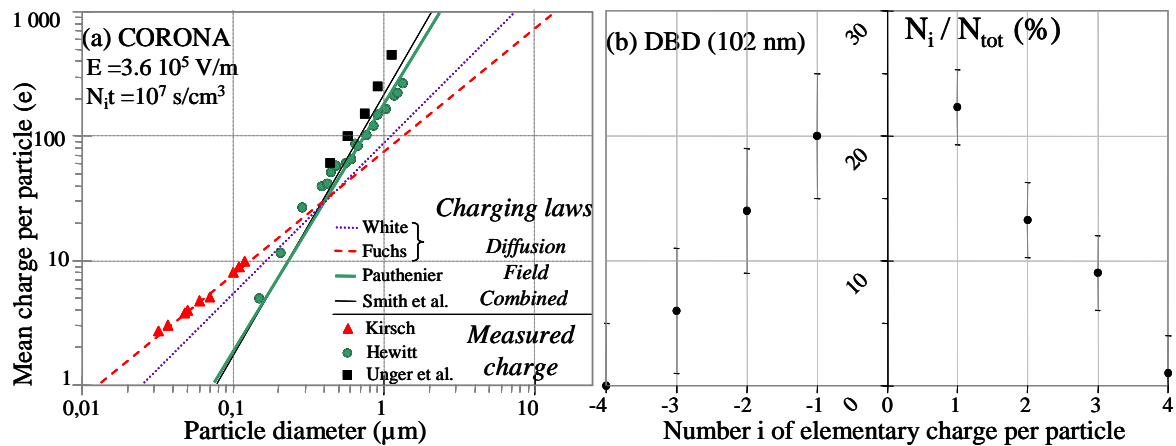


Figure 5: (a) Comparison of theoretical and measured mean number of charges by diffusion (White and Fuchs) and field (Pauthenier and Smith et al.) charging versus particle diameter [6], (b) Charge distribution in DBD charger ($F=20 \text{ kHz}$, $V_{\text{pp}}=17.5 \text{ kV}$ for + and 20 kV for -, with 15 ms transit in the DBD).

Taking advantage of tunable frequency, different DBD have been tested as aerosol chargers to reduce electro-collection [23][24][25], compared to corona chargers. The mean charge per particle (extrapolated from the collection efficiencies in the intermediate size range from 0.1 to $1 \mu\text{m}$) is positive and higher in DBD (20 kV peak-to-peak and $1\text{-}60 \text{ kHz}$ frequency) than in stationary ion density profiles of dc corona working at $N_i\tau$ product around 10^7s.cm^{-3} [23]. However, our first charge distribution on 102 nm particles of **Figure 5b** shows that for such small particles only charged by diffusion, the mean charge per particle extrapolated from electro-collection efficiency is over-estimated. Indeed, in this case, higher collection efficiency can result from turbulent mixing and/or additional charging mechanism for particles bigger than 30 nm , as well as thermophoresis from hotter gas to surface between filaments [6][26].

In DBD, thin and brief filaments (diameter $\sim 100\ \mu\text{m}$, duration $\sim 20\ \text{ns}$) are homogeneously distributed in space during two quarters of period. Each filament can be considered as a local brief and confined ion/electron source (cf. Figure 6, [6]). Indeed, charging by ions mainly occurs outside the bipolar plasma confined in the filamentary discharge i.e. in the ion clouds remaining in the gap after each filament due to surface polarization, for a time depending on geometry, voltage and frequency. In DBD, the net space charge as well as the mean of the resulting charge distribution (**Figure 5b**) is positive, due to faster collection of electrons and negative ions on the anode side of the filament.

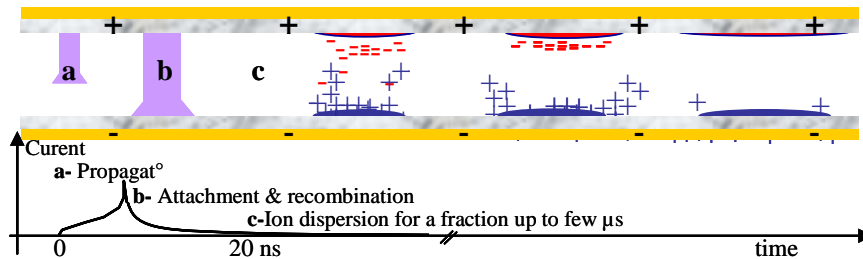


Figure 6: Filament development and ion distribution around a single filament during half a period

DBD is an alternative to corona discharges to charge particles efficiently with minimal losses. Indeed, the oxidation of metal electrodes as well as sparking, both producing particles and unstable discharges can be prevented. Moreover, electro-collection can be reduced in DBD, by working at ac-frequency above a few tens of kHz with similar charge than in coronae for particles charged by diffusion only (up to 100 nm), but with expected higher charge for intermediate and coarse particles (from 0.1 to 1 μm) also charged by field charging. Low frequency DBD with transit times shorter than the charging time (~ 5 periods, at least up to 9 kHz [23]), also leads to reduced charge and electro-collection [25].

4. NANO-MATERIALS PRODUCTION AND PROCESSING BY AP-PLASMA

For the production of nanoparticles from plasmas as well as for deposition in or after plasmas, charging and electro-thermal deposition have to be controlled.

4.1. Interest of plasma for applications of controlled kinematics of charged particles

Aerosol charging is involved in many applications such as electrostatic precipitation, coating, self-repulsion to preserve high interfacial areas, post-production particle assembly by Coulombian coagulation of bipolar aerosols and measurements based on electrostatic techniques. Depending on the application, high charge level, or reduced losses in the charger is required.

Recent advances in nanotechnology imply increasing efforts to control the charge distribution of aerosols for size measurement, sampling, transport, and material processing, especially for particles smaller than 100 nm. In this size range, only diffusion charging can account for the charging of nucleated particles. As in dc coronae, the charging of particles by repetitive ion sources in DBD is effective down to 10-30 nm, but partial charging of only a fraction of incoming particles is observed below 10 nm [11]. However, particle size measurement and film deposition including nanoparticles of controlled properties (size, composition and structure) are promising at least down to 10 nm.

Electro-collection may be prevented for aerosol size distribution measurements and for nano-materials production (cf. 4.2). Many aerosol instruments are based on defined charge-diameter relations with coronae, radioactive, UV or X-ray sources. Then particles are selected versus the size-dependant mobility [27]. DBD may be used as aerosol chargers for aerosol characterization; all the more that frequency of DBD can be tuned above a few kHz to limit electro-collection of particles compared to coronae. Electro-deposition of such ultra-fine nucleated nanoparticles ($< 100\text{nm}$) is prevented in dc and ac filamentary discharges due to poor charging efficiency with short transit time ($< 0.1\ \text{ms}$) and to poor collection efficiency in DBD at high frequency (10-100 kHz).

On the contrary, *when electro-collection is required* for film deposition, the charging by collection of ions is efficient only for particles bigger than a few nanometers. Hence, electro-collection of particles on surfaces is used for thin film deposition in 2.5 kHz DBD, with transit times in the DBD longer than the times of vapors formation, nucleation and growth above the minimum size to get charged [11].

Post-discharge collection: when particles have to be extracted from the plasma, thermophoretic and

diffusion deposition on cold post-discharge tubes and/or cooled substrates as well as space charge repulsion, have to be considered for accurate prediction of deposition positions and rates, as well as to calculate the real initial size distribution from post-discharge mobility selection and current measurements of collected charged particles (or particle concentration), for each mobility range.

4.2. Calibrated nanoparticle generator by AP plasma for standards

Standard reference aerosols are required to study size-dependant properties of nano-materials, as well as the indoor/outdoor transport to define the dispersion and deposition rates (e.g. for security norms of manipulation of nano-powders, exposition of people in industrial environment and for material aging). Besides, such low cost size-calibrated standard aerosols generator is also needed for the calibration of size measurement tools, which are under development. Figure 7 shows that « low energy » filament developing in DBD can be used to produce unimodal narrow size-distribution of nanoparticles.

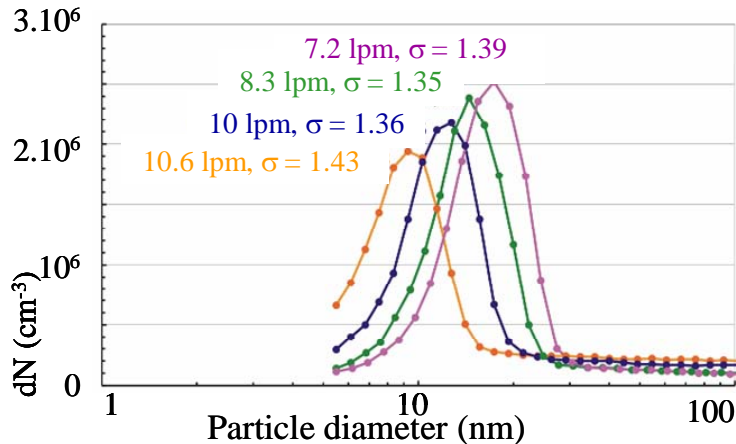


Figure 7: Size distribution and related geometric standard deviation (σ) produced by our DBD aerosol generator for different N_2 flow rates from 2 mm thick Alumina DBD (gap = 1 mm at 7 kV, 70 kHz), in collaboration with Prof. Weber from Clausthal University.

4.3. Focused/homogeneous deposition by controlled nucleation, growth and charging

Focused/ homogeneous deposition is achieved in AP Plasmas by controlling the charge, either directly in the plasma where particles are produced by nucleation or by post-production Plasma chargers [6]. Deposition of nucleated particles from plasma-gas interaction is used for pollution control (cf. 2.2) and coating, depicted here, while aerosol injection in plasma chargers is used for filtration by electrostatic precipitation (ESP) as well as for post-production sampling and assembly on surfaces [6].

To account for the size of particles included in the SiO_x film deposition from Silicon precursor, all smaller than 50 nm, similar size-dependent particle charging and electro-collection are involved in both filamentary and homogeneous DBD. Indeed, despite different charging conditions, similar films are formed closer to the precursor injection in filamentary than in homogeneous DBD. The higher energy density leads to faster formation, growth and charging of particles in filamentary than in homogeneous DBD, due to higher densities of active species for reactions producing vapors and nanoparticles, and of ions for particle charging [11].

Below 10 kHz, electro-collection reduces the production of vapors and nucleated particles from DBD, either by initial collection of high mobility clusters formed by ion-induced nucleation or by post-production charging by ion diffusion and photo-emission for 30 nm and bigger particles, for transit times above a few ms. At higher frequencies, turbulent mixing, additional charging mechanism and thermophoretic losses lead to higher collection efficiency in DBD than expected by electro-collection.

4.4. Composites

Finally, any material can be associated into composites by co-evaporation in sparks with different electrodes. Moreover, bi-metallic agglomerates made of mono-metallic nucleated primary nanoparticles from each electrode are produced in spark with two different electrodes. Hence, rapid and local nucleation occurs close to vapor sources, while coagulation leading to agglomerates occurs later. Resulting bi-metallic agglomerates could be melted to reach composite materials [1][3][7].

5. CONCLUSION

The interest of plasmas in aerosol processes lies on tunable properties (composition, size, structure and density) of aerosol that can be produced and processed in Atmospheric Pressure Electrical Discharges:

- Both energy density in the spot of discharge filaments and gas flow rate control the vapor flux from each filament (with voltage in asymmetric gap and with gap length in DBD), the subsequent particle concentration and growth by coagulation to produce nucleated nano-powders with tailored size.
- Any material can be produced by filamentary discharges (streamer and spark) on different surfaces
- High selectivity and vapors production rate lead to high purity particles from gaseous precursors.
- Controlled thermal gradient and cooling rate around the vapor source controls the particle structure,
- Fast coagulation occurs for $N_p > 10^7 \text{ cm}^{-3}$, so that nano-materials with size dependant properties can only be produced if coagulation is prevented either by immediate in line post-production processing or at concentration lower than 10^7 cm^{-3} , both possible with AP Plasmas.

Hence, aerosol with narrow size distribution can be produced to reach size-dependant properties of nano-materials with high specific surface area of any composition (polymer, multi-metal oxides and non-oxide Nitrides, Carbides and Borides) that can, then, be processed in powders, thin film or associated in composites by AP plasmas.

New non-thermal APED, such as the Micro-hollow Cathode, have been developed in the last decade and may be used to reach higher production rates in more homogeneous and larger volume plasmas.

APED can thus be considered as one of the missing links between the production goals and means in the challenging field of aerosol processes for new structural and functional materials either in powders for off-line processing, or in films, or in composite materials from integrated in-line processing.

ACKNOWLEDGMENTS

LIBS measurements have been performed by Frejafon E, Dutouquet C. and Amodeo T from INERIS

REFERENCES

- [1] Kodas T T and Hamnden-Smith M *Aerosol Processing of Materials* (New York: Wiley-VCH) (1999)
- [2] Tatoulian M et al *Chem. Materials*, **18**, 5860-5863 (2006)
- [3] Boulos M and Pfender E *MRS Bull.* **21**(8) 65-8 (1996)
- [4] Jidenko N et al. *J.Phys. D:Appl. Phys* **39-2** 281-293 (2006)
- [5] Petit M ;, et al *Rev. Scientific Instrument* **73-7** 2705-2713
- [6] Borra JP *J.Phys. D:Appl. Phys* **39-2** R19-R54 (2006)
- [7] Sano N et al. *Chemical Physics Letters* **368** 331-337 (2003)
- [8] Pratsinis S *Journal of Aerosol Science* invited conf. of EAC 07 (2007)
- [9] Mizuno et al. *IEEE Trans. Indust. Appl.* **35** 1284-8 (1999)
- [10] Odic E et al. ed E M Van Veldhuizen (New York: NOVA Science Publishers) 279-312 (2000)
- [11] Jidenko N et al. *J.Phys. D:Appl. Phys* **40 -14** 4155-4163 (2007)
- [12] J. Gonzales et al *J.Phys. D:Appl. Phys* **40** 2361-2374 (2007)
- [13] Byeon J H et al. *Journal of Aerosol Science* **39-10** 888-896 (2008)
- [14] Willeke K and Baron P *Aerosol Measurement* (New York: Ed Van Norstrand Reinhold) (1993)
- [15] Hinds W C *Aerosol Technology* 2nd edn (New York: Wiley) (1999)
- [16] White H.J *Trans. AIEE* **70** 1186-1191 (1951)
- [17] Fuchs N *Geofis. Pura Appl.* **56** 185-92 (1963)
- [18] Pauthenier MM, Moreau-Hanot M *J. Phys. Radium* **3** 590 (1932)
- [19] Cochet R 1961 *Colloque Int. la Phys. Forces Electrostat. et Leurs Application* **102** CNRS, Paris 331-338
- [20] Alonso M et al. *Journal of Aerosol Science* **29** 263-270 (1998)
- [21] Unger L et al. *J.Aerosol. Sce* **35-8** 965-979 (2004)
- [22] Stommel Y G and Riebel U *Journal of Aerosol Science* **35** 1051-1069 (2004)
- [23] Jidenko N. and Borra JP *J.Phys. D:Appl. Phys* **38-4** 617-620 (2005)
- [24] Kwon S-B et al. *J. of Nanopart. Research* **9-4** 621-630 (2006)
- [25] Byeon J H et al. *Journal of Aerosol Science* **39** 460-466 (2008)
- [26] Jidenko N. and Borra JP Hakone XI same proceeding (2008)
- [27] Biskos G. et al. *Aerosol Sci. & Techn.* **39-6** 527-541 (2005)